

## **SIMPLIFIED MODELING AND MEASUREMENT PROCEDURES FOR ELECTROMAGNETIC LAUNCHERS PERFORMANCES EVALUATION**

**Hocine Menana**\*

Research Institute of the French Naval Academy, CC 600-29240, Brest Cedex 9, France

**Abstract**—In this work, Simplified modeling and measurement procedures for capacitive driven electromagnetic launchers using magnetic armatures are presented. The modeling strategy is based on a successive solving of the circuit equation coupled to a 2D finite element (FEM) magnetostatic computation and the mechanical equation of the armature motion. This leads to a considerable time and memory space saving compared to a time domain magnetodynamic problem computation. The armature velocity is determined through the analysis of the time variation of the induced voltage, due to the armature remanent magnetization, in an auxiliary coil placed at the launcher extremity. The modelling and measurement strategies are implemented and tested on a laboratory developed coil-gun prototype. Modelling and measurement results are provided.

### **1. INTRODUCTION**

Electromagnetic launchers are of great interest for both the civil industry and military applications [1]. They have been proposed for airspace and air craft launch systems, replacing steam catapults, due to their advantages in terms of controllability, security, volume and lifetime [2–4]. Moreover, super velocities up to 8 Km/s can be reached with such devices [5]. Their design and optimization have attracted increasing interest of the scientific community during the past few decades.

The electromagnetic modelling of such devices requires solving a time domain magnetodynamic problem, coupled to the electrical circuit equation of the inductor and the mechanical equation of the

---

*Received 5 May 2013, Accepted 22 June 2013, Scheduled 27 June 2013*

\* Corresponding author: Hocine Menana (hocine.menana@ecole-navale.fr).

armature motion [6]. Several approaches have been used to solve this problem, such as the time domain finite element method [7, 8], the finite element-boundary element coupling [9] and the electrical filament circuit method which is commonly used [10–12]. In the first two approaches, the circuit equation has to be imposed, and unless using homogenization techniques [13], the mesh has to be dense in the inductor region; moreover, the meshing size is linked to the time discretization to ensure the convergence of the system. In the filament circuit approach, the circuit equation is implicitly taken into account; however, it leads to full matrices limiting the number of elements of the mesh even though the air region is not meshed in this case. Furthermore, its formulation may be complicated for non cylindrical geometries of the inductor and the armature.

In this work, we propose simplified modeling and measurement procedures for capacitive driven electromagnetic launchers using magnetic armatures. In the modeling procedure, the circuit equation is solved iteratively, coupled to a 2D FEM magnetostatic computation and the mechanical equation of the armature motion. This leads to a considerable time and memory space saving compared to a time domain magnetodynamic problem computation. The armature velocity is determined through the analysis of the time variation of the induced voltage, due to the armature remanent magnetization, in an auxiliary coil placed at the launcher extremity. The modelling and measurement strategies are implemented and tested on a laboratory developed coil-gun prototype. Modelling and measurement results are provided.

We start by describing the experimental setup and then we develop the modelling procedure. Results and discussions are given in the last section.

## 2. THE EXPERIMENTAL SETUP

The experimental setup and the electrical circuit model of the system are described in Fig. 1. It is a laboratory handmade coil-gun which consists of a coil wound over a non-conducting flyway tube, and powered by a 0.1 F/40 VDC capacitor. The capacitor is charged from the electric power grid via a transformer and a rectifier. A clamp-on amp probe connected to an oscilloscope is used to measure the current flowing in the launcher coil, and an auxiliary coil, situated at the flyway tube extremity and directly connected to a second oscilloscope, is used to measure the armature velocity. A schematic view of the coil-gun is given in Fig. 2, with the system parameters given in Table 1. These parameters have not been subject to a prior optimization. Notice that only the lengths of the auxiliary coil and that of the armature need to

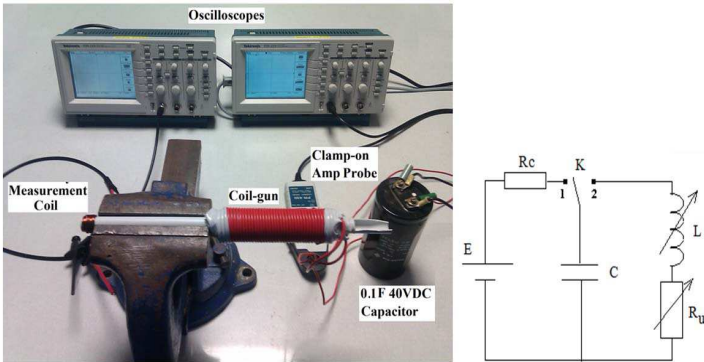


**Figure 1.** A picture view and the electrical circuit model of the experimental setup.

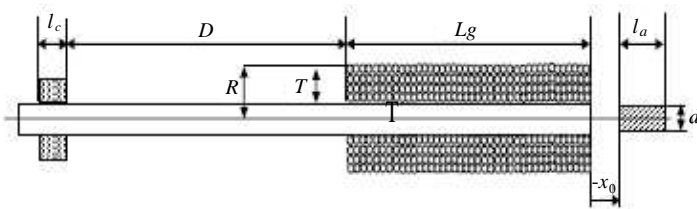


**Figure 2.** Schematic view of the coil-gun.

**Table 1.** The system parameters.

Component	Parameters values
Launcher coil	$R = 19 \text{ mm}$ , $T = 11 \text{ mm}$ , $Lg = 130 \text{ mm}$ , Number of turns = 160, Electrical resistance $R = 0.21 \Omega$
Armature	Cylindrical form, $l_a = 24 \text{ mm}$ , $d = 12 \text{ mm}$ , Steel material, Mass ( $m$ ) = 20 g
Capacitor	0.1 F/40 VDC
Amp probe	10 mV/A
Auxiliary coil	$l_c = 14 \text{ mm}$ , Number of turns = 110 (thin copper wire), Distance from the launcher coil ( $D$ ) = 150 mm

be known for the armature velocity measurement.

### 3. THE MODELING STRATEGY

In the electrical circuit model, the inductance  $L$  and resistance  $R_u$  vary with the armature motion. At  $t = 0$  the capacitor  $C$  is completely

charged and the switch  $K$  passes to the position 2, closing the  $R_u LC$  circuit. The expression of the time variation of capacitor voltage  $V_c$  is given by (1), where the resistance  $R_u = R + udL/dx$  involves the coil wire resistance  $R$ , the armature velocity  $u$  and the inductance derivative according to the direction  $x$  of the armature motion.

$$V_c = R_u C \frac{dV_c}{dt} + LC \frac{d^2 V_c}{dt^2} \quad (1)$$

Solving (1), the  $i$ th values of the capacitor voltage  $V_c^i$  and the current  $I_c^i$  in the circuit, at the  $i$ th value of the time  $t^i = t^{i-1} + \Delta^i t$ , where  $\Delta^i t$  is the  $i$ th time step, are given by (2) and (3), for the  $i$ th value  $R_u^i$  of the resistance  $R_u$  and the  $i$ th value  $L^i$  of the inductance  $L$  ( $i = 1, 2, \dots, n$ ).

$$V_c^i = K_1^i e^{\alpha_1^i t^i} + K_2^i e^{\alpha_2^i t^i} \quad (2)$$

$$I_c^i = -C \left( K_1^i \alpha_1^i e^{\alpha_1^i t^i} + K_2^i \alpha_2^i e^{\alpha_2^i t^i} \right) \quad (3)$$

with:

$$\begin{cases} K_1^i = -\frac{\alpha_2^i V_{c0}}{\alpha_1^i - \alpha_2^i} \\ K_2^i = \frac{\alpha_1^i V_{c0}}{\alpha_1^i - \alpha_2^i} \end{cases} \quad (4)$$

$$\begin{cases} \alpha_1^i = -\frac{R_u^{i-1} C + \sqrt{(R_u^{i-1} C)^2 - 4L^{i-1} C}}{2L^{i-1} C} \\ \alpha_2^i = -\frac{R_u^{i-1} C - \sqrt{(R_u^{i-1} C)^2 - 4L^{i-1} C}}{2L^{i-1} C} \end{cases} \quad (5)$$

$$R_u^i = R + u^{i-1} \frac{L^i - L^{i-1}}{x^i - x^{i-1}} \quad (6)$$

The  $i$ th values of the velocity and position of the armature are evaluated as follows:

$$x^i = \frac{1}{2} \frac{F^{i-1}}{m} (\Delta^i t)^2 + u^{i-1} \Delta^i t + x^{i-1} \quad (7)$$

$$u^i = \frac{F^{i-1}}{m} \Delta^i t + u^{i-1} \quad (8)$$

In (7) and (8),  $m$  is the armature mass and  $F^{i-1}$  is the total force acting on the armature at the position  $x^{i-1}$ . The total force is the sum of the magnetic force  $F_m$ , the drag force  $F_d$  and the armature weight  $m \cdot g$  in the case of a vertical launch, where  $g$  is the gravity.

$$F^i = F_m^i - F_d^i \pm m \cdot g \quad (9)$$

The expression of the drag force is given by (10) [14], where  $\rho$  is the air density in  $\text{kg/m}^3$ ,  $u^i$  is the  $i$ th value of the armature velocity

in m/s,  $S_f$  is the frontal surface of the armature in  $\text{m}^2$  and  $C_x$  is the dimensionless drag coefficient.

$$F_d^i = 0.5 \rho (u^i)^2 S_f C_x \quad (10)$$

Starting from the initial values ( $V_c^0, L^0, x^0, u^0, I_c^0 = 0, F^0 = 0$  or  $\pm m \cdot g, R_u^0 = R$ ) at  $t = 0$ , we evaluate at each time step the previous equations in the following order:  $(\alpha_1^i, \alpha_2^i) \rightarrow (K_1^i, K_2^i) \rightarrow I_c^i \rightarrow (L^i, F_m^i)$  *numerically by solving a magnetostatic problem, using the current  $I_c^i$*   $\rightarrow F^i \rightarrow u^i \rightarrow x^{i+1} \rightarrow R_u^{i+1}$ .

## 4. RESULTS AND DISCUSSION

### 4.1. Experimental Results

For a launch corresponding to the initial position ( $x_0 = 0$ ) of the armature, we measured the time variations of the current in the coil-gun and the voltage induced in the auxiliary coil, given by Figs. 3(a) and (b) respectively. We can notice that the current reaches a peak value of 150 A at  $t = 2$  ms, and decays exponentially to zero, reached at about  $t = 0.1$  s. The induced voltage in the auxiliary coil is the time derivative of the magnetic flux created by the magnetized armature moving through it. Considering that the magnetization of the armature is constant during its movement through the coil, the induced voltage is proportional to the coil inductance derivative. The shape of the voltage signal depends on the ratio of the lengths of the armature and the coil. As the armature and coil lengths are close in this case, the induced voltage appears as a sinusoid. For the armature velocity evaluation, one can use the extrema and the zero crossing times of the induced voltage, knowing the corresponding positions of the armature. In this

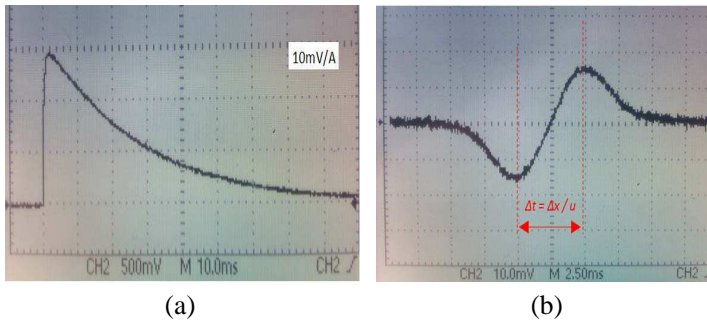


**Figure 3.** The measured: (a) current in the launcher coil and (b) voltage in the auxiliary coil.

work, we used the time between the extrema; the distance covered by the armature between the two peaks of the voltage (Fig. 3(b)) has been evaluated numerically by a finite element calculation scheme using the Finite Element Method Magnetics (FEMM) free software. The calculation gives  $\Delta x = 18$  mm, and thus the armature velocity is:  $u = \Delta x / \Delta t = 3.6$  m/s ( $\Delta t = 5$  ms, identified in Fig. 3(b)).

## 4.2. Electromagnetic Model Validation

A coupling between Matlab and FEMM software is achieved to implement the numerical model. In FEMM, the magnetostatic part of the problem is calculated. The Laplace equation ( $\Delta A = -\mu J$ ), involving the magnetic vector potential  $A$ , the current source density  $J$  and the magnetic permeability  $\mu$ , is solved using a 2D axisymmetric finite element calculation. The Dirichlet boundary condition ( $A = 0$ ) is applied on the external frontier. The magnetic energy is used to evaluate the inductance of the launcher coil and the virtual work method is used to evaluate the electromagnetic force acting on the armature. A flow diagram, given by Fig. 4, describes the modeling procedure. The values of the parameters used in Equation (10) are:  $\rho = 1.2$  kg/m<sup>3</sup>,  $C_x = 1$  and  $S_f = 2.8274 \times 10^{-5}$  m<sup>2</sup> which is the frontal surface of the armature.

The finite element model geometry, mesh, and the calculated

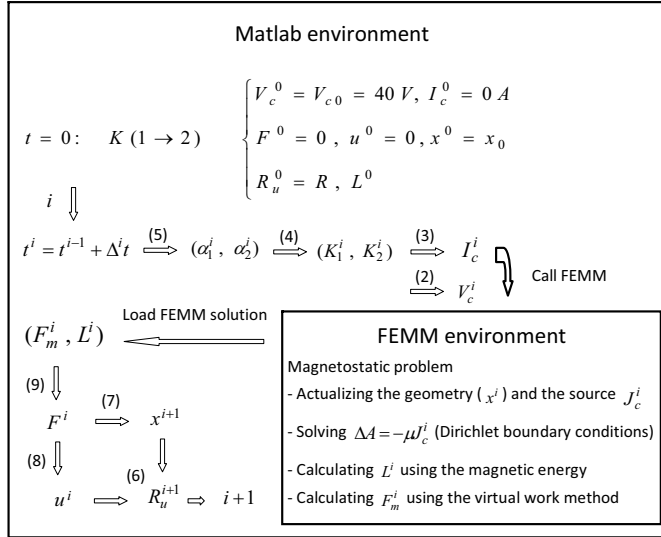


**Figure 4.** The modeling procedure.

magnetic field, at the position ( $x_0 = 0$ ) of the armature, are shown in Fig. 5. The implemented program is executed on 100 points of calculation with a time step of 1 ms. The CPU time is 96 seconds on a 2.4 GHz and 3Go Ram PC. At each time step, the current in the launcher coil and the armature velocity are calculated by (3) and (8) respectively. The coil-gun inductance and the electromagnetic force are calculated numerically in FEMM. The total force acting on the armature is obtained by (9), taking account of the electromagnetic force and the drag force given by (10). The obtained values are plotted as functions of the time.

In Fig. 6, a comparison between the measured and calculated currents in the coil-gun, corresponding to the initial position ( $x_0 = 0$ ) of the armature, is presented. A good agreement is shown between the two results over the entire time interval. Fig. 7 shows the time variation of the coil-gun inductance which can be converted to the space variation by introducing the armature velocity. The coil-gun inductance increases as the armature penetrate into it, reach its maximum at the middle position and then decreases when the armature tends to quit the coil-gun. This time variation is not symmetric since

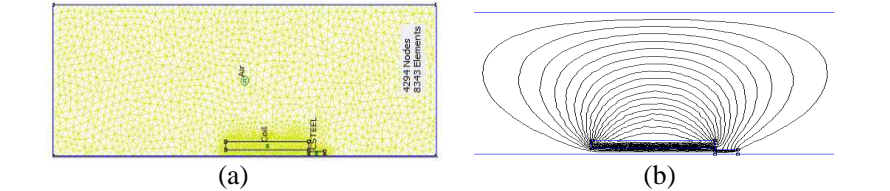


**Figure 5.** (a) 2D FEM geometry, mesh and (b) magnetic field distribution ( $x_0 = 0$ ).

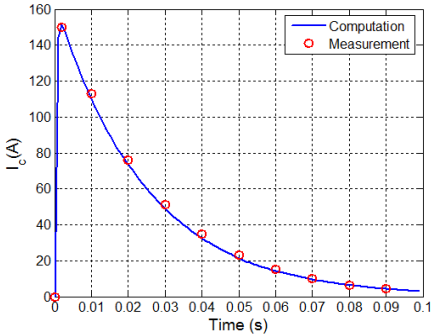


**Figure 6.** Comparison between the calculated and measured currents.

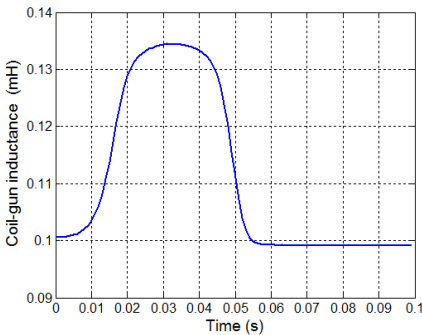


**Figure 7.** Time variation of the coil-gun inductance.

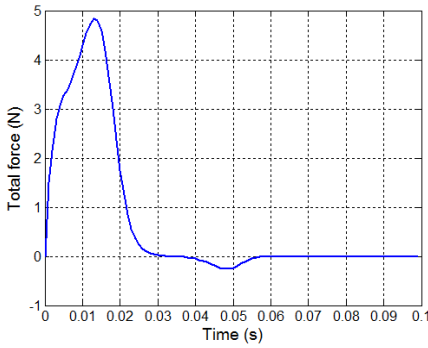


**Figure 8.** Time variation of the total force applied on the armature.

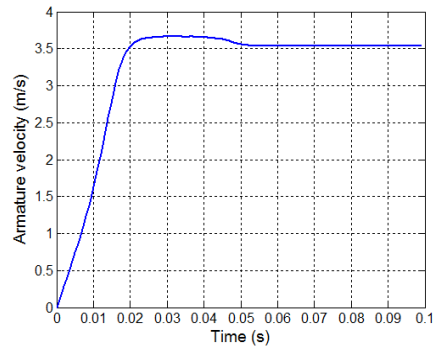


**Figure 9.** Time variation of the armature velocity.

the velocity of the armature varies as it passes through the coil-gun. It is the variation of the inductance, combined with the current that is responsible for the magnetic force creation, as shown in Fig. 8. As the current is not nil when the inductance decreases, a restoring force is applied on the armature, which tends to slow it down as shown in Fig. 9. At  $t = 0.055$  s, the armature leaves the coil-gun, carrying its motion in the flyway tube and slowed down by the drag force. The calculated velocity at the auxiliary coil position is  $u = 3.5$  m/s which is close to the measured one (3.6 m/s); the relative error is less than 2.8%. This error may be particularly due to an error in the initial position of the armature which is not well determined experimentally.

## 5. CONCLUSION

A simplified modeling and measurement procedures to evaluate the performances of coil-gun launchers with magnetic armatures are presented. Despite the simplicity of these procedures, a good accuracy is achieved. The modeling approach results in a considerable gain in time and memory space compared to the common approaches. Indeed, it is easier to integrate a numerical modeling in circuit equations solving than integrating circuit equations in a numerical modeling. The nonlinearity of the magnetic properties can be easily taken into account with no significant increase in the computation time. Notice that one can also use semi-analytical models to compute the magnetostatic part of the problem, such as the model presented in [15]. The measurement procedure is very simple and inexpensive to implement. The simplicity and the rapidity of these approaches make them suitable to be used in the design and optimization, as well as in education and trainings.



The use of the presented modeling and measurement procedures is however limited to coil-guns using magnetic armatures. As the eddy currents and the skin effect in the armature are not considered, further investigations are needed to check whether the obtained accuracy does not result from a compensation of modeling and measurement errors, though the most influent parameter in such system is the air-gap between the coil and the armature, which define the magnetic field strength in the latter. Indeed, unless the armature is magnetically saturated, its permeability is seen as infinite compared to the air region, and the magnetic field will be concentrated essentially in the rear portion of the latter; thus the skin effect has not the same influence as in purely conductive armatures. As no traveling wave is generated in the coil-gun, the eddy currents in the armature do not contribute to the axial force generation, but they must be taken into account to achieve the energy balance which is not ensured in the proposed modeling approach. One can eventually correct the model to take account of the skin effect by considering, at each iteration in the magnetostatic computation, only a portion of the armature thickness starting from the surface, with the armature mass kept unchanged. This portion of the armature thickness would be the product of the time and the velocity of the electromagnetic field diffusion in the considered material. The eddy current in the armature could also be computed in a weak form by a backward time derivative of the average value of the magnetic vector potential obtained by the magnetostatic computation, under the condition of applying a small time step.

## ACKNOWLEDGMENT

The author thanks the French Naval Academy Student Officers: A. Vershae and L. Morvan, for their contribution to the experimental setup realization.

## REFERENCES

1. Vottis, P. M., M. Cipollo, E. Kathe, Z. Zabar, E. Levi, and L. Birenbaum, "Use of electromagnetic coil launcher to increase muzzle velocity of conventional cannons," *IEEE Trans. Magn.*, Vol. 33, No. 1, 190–194, 1997.
2. Hasirci, U., A. Balikci, Z. Zabar, and L. Birenbaum, "Concerning the design of a novel electromagnetic launcher for earth-to-orbit micro- and nanosatellite systems," *IEEE Trans. on Plasma Science*, Vol. 39, No. 1, 498–503, 2011.
3. Li, L., M. Ma, B. Kou, and Q. Chen, "Analysis and optimization

- of slotless electromagnetic linear launcher for space use,” *IEEE Trans. on Plasma Science*, Vol. 39, No. 1, 127–132, 2011.
4. Doyle, M. R., D. J. Samuel, T. Conway, and R. R. Klimowski, “Electromagnetic aircraft launch system — EMALS,” *IEEE Trans. Magn.*, Vol. 31, No. 1, 528–533, 1995.
  5. Balikci, A., Z. Zabar, L. Birenbaum, and D. Czarkowski, “On the design of coilguns for super-velocity launchers,” *IEEE Trans. Magn.*, Vol. 43, No. 1, 107–110, 2007.
  6. Zouia, M., H. Mohellebi, and M. Abdellah, “Electric-magnetic-mechanical coupled model for analyzing dynamic characteristics with feeding effects of linear induction launcher,” *IASME Transactions*, Vol. 1, No. 2, 235–240, 2004.
  7. Zou, B., Y. Cao, J. Wu, H. Wang, and X. Chen, “Magnetic-structural coupling analysis of armature in induction coilgun,” *IEEE Trans. on Plasma Science*, Vol. 39, No. 1, 65–70, 2011.
  8. Manna, M. S., S. Marwaha, and A. Marwaha, “Performances optimization of linear induction motor by eddy current and flux density distribution analysis,” *Journal of Engineering Science and Technology*, Vol. 6, No. 6, 769–776, 2011.
  9. Liu, S., J. Ruan, and Y. Zhang, “Application of FE-BECM in field analysis of induction coil gun,” *IEEE Trans. on Plasma Science*, Vol. 39, No. 1, 94–99, 2011.
  10. Zhang, Y., Y. Wang, and J. Ruan, “Capacitor-driven coil-gun scaling relationships,” *IEEE Trans. on Plasma Science*, Vol. 39, No. 1, 220–224, 2011.
  11. Liu, S., J. Ruan, Y. Peng, Y. Zhang, and Y. Zhang, “Improvement of current filament method and its application in performance analysis of induction coil gun,” *IEEE Trans. on Plasma Science*, Vol. 39, No. 1, 382–389, 2011.
  12. Lei, B., X. Guan, Z. Li, and B. Zhi, “Performance analysis of single inductive coil driver,” *IEEE Trans. on Plasma Science*, Vol. 39, No. 1, 53–58, 2011.
  13. Sabariego, R. V., P. Dular, and J. Gyselinck, “Time-domain homogenization of windings in three-dimensional finite element,” *Proceedings of COMPUMAG’2007*, 1107–1108, Aachen, Germany, 2007.
  14. Hertz, B. P. and P. R. Ukrainetz, “Auto-aerodynamic drag-force analysis,” *Experimental Mechanics*, Vol. 7, No. 3, 19A–22A, 1967.
  15. Lubin, T., K. Berger, and A. Rezzoug, “Inductance and force calculation for axisymmetric coil systems including an iron core of finite length,” *Progress In Electromagnetics Research B*, Vol. 41, 377–396, 2012.